KSCE Journal of Civil Engineering (2018) 22(7):2371-2383
DOI 10.1007/s12205-017-1437-5

Structural Engineering
pISSN 1226-7988, eISSN 1976-3808
www.springer.com/12205

The Effect of FEM Mesh Density on the Failure Probability Analysis of Structures

Alireza Ghavidel*, S. Roohollah Mousavi, and Mohsen Rashki*****

Received August 25, 2016/Revised Jaunary 19, 2017/Accepted July 5, 2017/Published Online September 11, 2017

Abstract

In the analysis of finite elements, mesh density can highly influence the accuracy of the results. Hence, researchers consider the determination and refinement of mesh an attractive issue. However, the subject has not been suitably investigated for the reliability evaluation of structures. This paper investigates the effects of mesh density on the reliability evaluation and the reliability-based sensitivity of structures. For this purpose, two common engineering problems modeled by Finite Element Method (FEM), with different mesh densities and their reliability results determined by Monte Carlo simulation and polynomial Response Surface Methodology (RSM). The analytical solutions to the proposed problems were present in the literature. Hence, the effects of the FEM mesh densities on the reliability results could be compared with the theoretical results. The outcomes based on the FEM results showed that RSM can very accurately evaluate the performance of these structures. However, the main achievement of the study was the finding that though a determined mesh density can be considered acceptable from the deterministic analysis viewpoint, its employment in reliability analysis could produce 100% error in estimating the failure probability of a structure.

Keywords: *finite element method, mesh density, reliability analysis, response surface method*

1. Introduction

Over the last 50 years, the Finite Element Method (FEM) has evolved to a point that it is now a commonly applied computer method in engineering analysis. It is used to simulate and evaluate the performance of structures and mechanical components. In Finite Element Analysis (FEA), the mesh density and quality highly affect the accuracy of the results and the required computing time. According to the FEA theory, models with a fine mesh often yield highly accurate results, but these may take longer to be computed. In contrast, coarse-meshed models may lead to less accurate results, but these also need less time to be computed. Hence, a higher mesh number is often employed when high accuracy is needed. Hence, the foremost problem is to choose the proper mesh density so that the models yield accurate FEA results in as little computing time as possible. Scholars of different sciences have done a lot of research in the field of deterministic analysis to achieve the best accuracy (Moxey *et al.*, 2015; Hu and Zhang, 2016). Brown (1981) introduced a non-interactive computer method, which tried to produce a good mesh with the minimum input data, using conformal mapping. Dyck *et al.* (1992) presented a system that used a neural network to predetermine the mesh density. Their system "learns" how to mesh from the examples of ideal meshes. When trained, the system computes the mesh density if the geometric and material descriptions of a device are given. Idelsohn and Onate (2006) assessed the advantages and disadvantages of mesh-free methods compared with standard-mesh ones. Also, some scholars have investigated the effects of mesh density on the results of the analysis, or compared the results of the FEA and the experimental data (Li *et al.*, 2016; Yao *et al.*, 2016; Perillo-Marcone *et al.*, 2003; Zmudzki *et al.*, 2008). Ashford and Sitar (2001) evaluated the accuracy of computed stress distribution near the free surface of vertical slopes as a function of the element size. A parametric study was taken into account to compare the stresses computed using FEM to those obtained from a physical model. Waide *et al.* (2004) used both experimental and finite element methods to investigate the load-transfer characteristics of two types of cemented hip replacements with a fibrous tissue layer. They accepted 15% difference between the experimental and the FE models. Studies on spinal segments have suggested that mesh convergence, by changing < 5% in the solution, is adequate (Jones and Wilcox, 2008). Gray *et al.* (2008) introduced the FE models of a human cadaveric tibia, and validated them against the results obtained from a comprehensive set of experiments. They showed that their FE models had a good agreement with the experimental

*MS.c Student, Civil Engineering Dept., University of Sistan and Baluchestan, Zahedan, Iran (E-mail: a.r.ghavidel@pgs.usb.ac.ir)
**Assistant Professor, Civil Engineering Dept., University of Sistan and Baluchestan, Zahedan, Iran (E-mail: s.r.mousavi@eng.usb.ac.ir)
***Assistant Professor, Dept. of Architecture Engineering, University of Sistan and Baluchestan, Zahedan, Iran (Corresponding Author, E-mail: Mrashki@eng.usb.ac.ir)

results with an R^2 value of 0.98 and 0.97 respectively. Roth and Oudry (2009) made a presentation on the influence of mesh density on an FE model under dynamic loading. They concluded that the mesh has a great influence on simple models. For complex models, the minimum number of elements according to the loading case would be necessary. Li *et al.* (2010) investigated the sensitivity of structural responses and rib fractures to mesh density, cortical thickness, and material properties. They accepted some percent of error for coarse-meshed models in their study.

The application of FEA, however, is not limited to the deterministic analysis of structures or mechanical systems. FEM is popular for the probabilistic analysis and reliability-based design optimization of systems. Consequently, selecting the suitable mesh density becomes more problematic when it comes to the reliability evaluation of a structure or mechanical system to determine the performance of which requires FEA. However, this paper is not concerned with the importance of mesh density in this field. Its main purpose is to investigate the effect of mesh density on the reliability evaluation of structures and the employed failure limit in reliability analysis. To do the reliability analysis, two engineering problems a plate rested on an elastic foundation and a cylindrical storage tank were used. Common reliability methods were used to evaluate the safety level. The Response Surface Methodology (RSM) was employed as a substitute to reduce the computation time and cost. Section 2 presents a review of the employed reliability method and RSM. The employed examples, computation results, and conclusions are presented in sections 3 and 4 respectively.

2. Reliability Analysis Methods and Response Surface Methodology

In structural reliability, the event of a component's failure is usually described in terms of a limit-state function that defines the boundary between the failure and the safety of its performance. The basic problem in structural reliability theory is the computation of the multifold probability integral as a probability of failure (*PF*), which is defined as:

$$PF = \text{Prob}\left[G(X) \le 0\right] = \int_{G(X)\le 0} f(X)dX \tag{1}$$

in which $X = [X_1, \ldots, X_n]^T$ with the superscript T = transpose. X is a vector of random variables representing uncertain structural quantities, such as loads, environmental factors, material properties, and structural dimensions. The functions $G(X)$ and $f(X)$ respectively denote the limit state function and the joint Probability Density Function (PDF) of X. $G(X) \le 0$ represents the domain of integration that covers the failure set (Zhao and Ono, 2001).

The proposed equation is generally difficult to evaluate, especially when the number of random variables is high, or the failure regions have complicated shapes (Zhao and Ono, 2001). Therefore, various simulation and approximation methods were adopted to assess the failure probability briefly reviewed in this section.

2.1 Approximation Reliability Methods

First-Order Reliability Methods (FORMs) are one of the most accepted computational methods to calculate Eq. (1) (Nowak and Collins, 2000; Ghohani-Arab and Ghasemi, 2015). According to these methods, the limit-state surface in the standard normal space (u space) is replaced with the tangent plane at the point that has the minimum distance from the origin. In that case, the first-order estimation of the *PF* is $P_f \approx \Phi(-\beta)$, where β, denoting the reliability index, is the minimum distance from the origin, and $\Phi(.)$ denotes the standard normal cumulative probability. In the Second-Order Reliability Methods (SORMs), the limit-state surface in the standard normal space is fitted to a second-order surface, which is usually a paraboloid (Der kiureghian and Ke, 1998).

The main effort in the FORM or the SORM is to find out the minimum distance point(s) from the origin in the standard normal space, denoted as u^*, on the limit-state function (G). This is formulated as a constrained optimization problem (Der kiureghian and Ke, 1998):

$$\begin{aligned} &\text{Minimize } |u| \\ &\text{Subject to } G(u)=0 \end{aligned} \tag{2}$$

The FORM results are accurate for engineering purposes when the limit-state function is moderately linear around u^*, and the random variables are normally distributed (Di Sciuva and Lomario, 2003; Lopez *et al.*, 2014).

2.2 Simulation-based Reliability Methods

The key step in the simulation methods is to generate samples, and evaluate the performance function for each generated sample. The Monte Carlo Simulation (MCS) is one of the most accurate and robust simulation methods for approximating the *PF* (Melchers, 1999). In this method, the *PF* is defined as the ratio of the number of samples in the failure region (n_f) to the total number of samples (N). The samples generated in an MCS for each variable are based on the respective PDFs. Most of the samples are generated about the means, and are proportionate to the respective standard deviations.

$$P_f = \int \ldots \int I[G(x) < 0] f_x(x) dx \approx \frac{1}{N}\sum_{i=1}^{n} I[G(x_i) < 0] \approx \frac{n_f}{N} \tag{3}$$

In the above equation, f_x is the PDF of the parameters, and "I" is the counter vector that is 1 in the failure region, and 0 in the safe region (Melchers, 1999).

Despite its high accuracy, this method cannot be directly applied to many engineering problems, especially those with a low probability of failure, and FE problems, due to the time-consuming approach and computing cost (Rashki *et al*., 2012; Hurtado *et al*., 1998).

Hence, as an improved sampling strategy, the Latin Hypercube Sampling (LHS) method has been developed for a reliable approximation of the stochastic properties (Helton and Davis, 2003; Hamdia *et al*., 2015; Pasbani Khiavi, 2016). In this method, the design space of variable X_i is subdivided into N equal probable intervals D_m:

$$P[X_i \in D_m]; \quad i = 1,...,k; \quad m = 1,...,N \tag{4}$$

in which N and k are the number of samples and the number of variables respectively.

2.3 Response Surface Methodology (RSM)

The straightforward solution to solve the inefficiency problem of MCS is to employ a proper meta-model (Xu *et al.*, 2016). RSM has been a key development in structural reliability analysis. Box and Wilson introduced it in 1954. In 1989, Faravelli first proposed its application in structural reliability analysis. RSM is highly proper for cases in which the closed-form expression for the performance function is not known, and needs to be evaluated by numerical methods like the FE method.

The goal of RSM is to replace $G(x)$ in Eq. (1) by an equivalent function $G^*(x)$, in which the computational procedures can be simplified (Bucher and Bourgund, 1990). In this work, a polynomial-type function is suggested as:

$$G^*(X) = a + \sum_{i=1}^{n} b_i X_i + \sum_{i=1}^{n} c_i X_i^2 + \sum_{i=1}^{n-1} \sum_{j=i+1}^{n} d_{ij} X_i X_j \tag{5}$$

in which x_i, $i = 1, \ldots, n$ are the basic variables, and the parameters a, b_i, c_i, d_{ij}, have to be determined. The coefficients of the function $G^*(X)$ are determined by the regression coefficients (Myers *et al.*, 2009).

2.4 Reliability-based Sensitivity Analysis

Besides reliability analysis, researches often wish to obtain reliability-based sensitivity results to rank the random variables of the problem based on their importance. The main objective of reliability-based sensitivity analysis is to study the influence of probabilistic model parameters on the reliability of a given structural system. In the context of this work, reliability sensitivity is defined as the partial derivation of the failure probability with respect to the distribution parameters of the uncertain structure parameters. Formally, the sensitivity of the failure probability, with respect to a distribution parameter p (which can be the mean or the standard deviation of each parameter), can be evaluated from (Jensen *et al*., 2015):

$$\begin{aligned} &\frac{\partial P_f}{\partial p} = \int I[G<0] f_{x(p)} dx \\ &\int I[G<0] \frac{\partial f_{x(p)}(x)}{\partial p}(x)dx = \int I[G<0] \frac{\partial f_{x(p)}(x)}{\partial p} \frac{1}{f_{x(p)}(x)} f_{x(p)}(x)dx \end{aligned} \tag{6}$$

In the above formula, f_x is the PDF of the parameters, and "I" denotes the counter vector defined in Eq. (3).

In this paper, the reliability analyses of a plate on an elastic foundation and a cylindrical storage tank were investigated to assess the effect of mesh density.

3. Mesh Densities' Effect on the Reliability Analysis of Engineering Problems

Two common engineering structures were chosen to assess the effect of mesh density on the reliability analysis. First, a plate on an elastic foundation is investigated in detail. Then, the reliability evaluation of a cylindrical storage tank is presented.

3.1 Plate on an Elastic Foundation

Plates on an elastic foundation have widespread application in the designing of mechanical systems and other engineering purposes. Some examples are the bottom plates of hydraulic structures and the surface plates of highways and runways. In this section, a one-inch thick infinitely large plate, resting on the Winkler foundation, was modeled to investigate the effect of mesh density on the reliability evaluation of the structure. The reason for the selection was that an implicit performance function for this problem was presented in (Timoshenko and Woinowsky-Krieger, 1959). That could be considered as a reference value for the validation of the FEA results. Fig. 1 shows the structure. The maximum plate deflection at the point load location (Δ_{plate}) is presented as:

$$\begin{aligned} &\Delta_{plate} = \frac{P\lambda^2}{8K} \\ &\lambda^4 = \frac{K}{D} \\ &D = \frac{Et^3}{12(1-\upsilon^2)} \end{aligned} \tag{7}$$

in which D is the flexural rigidity of the plate; K is the sub-grade modulus; t is the thickness of the plate; E is the modulus of elasticity of the plate; and υ is the Poisson's ratio of the plate. As Fig. 1 shows, for the FEA of the problem, the infinitely large plate was modeled as 300 inches long and 300 inches wide, at the center of which a point load was applied. The Δ_{plate} was evaluated by FEA. Eq. (7) was used to validate the results achieved by FEA.

The material used for the analysis was steel with a modulus of elasticity $E = 29{,}000$ kip/in^2 and Poisson's ratio $\upsilon = 0.3$. The applied load was a 50 kips point load on the center of the plate (P).

Ten kinds of mesh densities were used to model the plate. The obtained results were compared with the analytical solution presented in Eq. (7). The models were analyzed using FEA software, namely, SAP2000. As mentioned before, in FEM, a major issue is to choose the best mesh density. It is often achievable by studying the convergence history of different mesh sizes (rough to fine) to a steady solution and Grid Convergence Index (GCI). When the difference of the results is lower than a certain value, the mesh density could be desirable for FEA

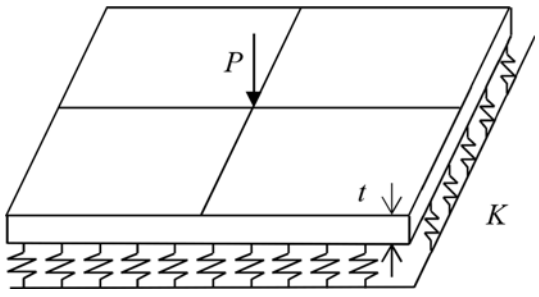

Fig. 1. Plate with Point Load

Table 1. Mesh-convergence Evaluation by the Analysis of 10 Models with Different Mesh Densities

Number of elements (length × width × height)	$\lvert \Delta_{plate} \rvert$ (inch)	The percent difference between a model and the previously analyzed model
10×10×1	0.039	----------
20×20×1	0.087	55.72%
30×30×1	0.123	28.97%
40×40×1	0.145	15.10%
50×50×1	**0.158**	8.11%
60×60×1	**0.165**	**4.56%**
70×70×1	0.170	2.72%
80×80×1	0.173	1.71%
90×90×1	0.175	1.13%
100×100×1	0.176	0.78%
Analytical solution	0.178	----------

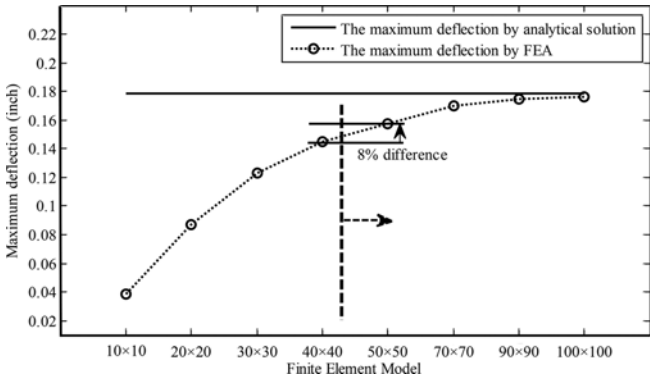

Fig. 2. The Convergence of FE Models to the Theoretical Solution

purposes. Table 1 and Fig. 2 show the proposed step. As Table 1 shows, the error percentage of the maximum deflection (Δ_{plate}) between the 50 × 50 × 1 and 60 × 60 × 1 (length × width × height) models is about 5%. The finer meshes have a lower percentage of difference with the models analyzed before them. Hence, the 50 × 50 × 1 model and those with a higher number of elements seem to be acceptable for FEA. Also, the GCI of the plate has an acceptable range of percentage for the 50 × 50 × 1 model and those after it. Hence, according to the literature (Jones and Wilcox, 2008; Li *et al.*, 2010) and as presented in Fig. 2, models that are after the dotted line can provide reliable results.

Of the 10 models, those with 50 × 50 × 1, 70 × 70 × 1, 90 × 90 × 1, and 100 × 100 × 1 meshes (named A, B, C, and D respectively) were selected to analyze the effect of mesh density on the reliability analysis of the plate. Two models are presented in Fig. 3.

For each model, one failure mode (exceeding the maximum allowable deflection) was defined as:

$$G = \Delta_{allowable} - \Delta_{plate} \tag{8}$$

In the above formula, G is the limit-state function, $\Delta_{allowable}$ is the failure limit, and Δ_{plate} could be each of the functions obtained by the RSM for the models with different mesh densities. Or, it could be the analytical function resulting from Eq. (7).

The random variables of the problem were the sub-grade modulus (K), the point load (P), and the modulus of elasticity (E) of the plate, which have been shown in Table 2. As an accurate reliability method, MCS is considered to solve this structural reliability problem. To reduce the computation time during MCS-based reliability analysis, the performance function (considered implicit in this state) was estimated by a two-order polynomial response surface function, named $G^*(K, P, E)$, as:

$$G^*(K,P,E) = a + b_1.K + b_2.P + b_3.E + c_1.K^2 + c_2.P^2 + c_3.E^2 + d_{12}.K.P + d_{13}.K.E + d_{23}.P.E \tag{9}$$

in which K, P, and E are variables, and a, b_1, b_2, b_3, c_1, c_2, c_3, d_{12}, d_{13}, and d_{23} are the coefficients of the function. To ensure that the

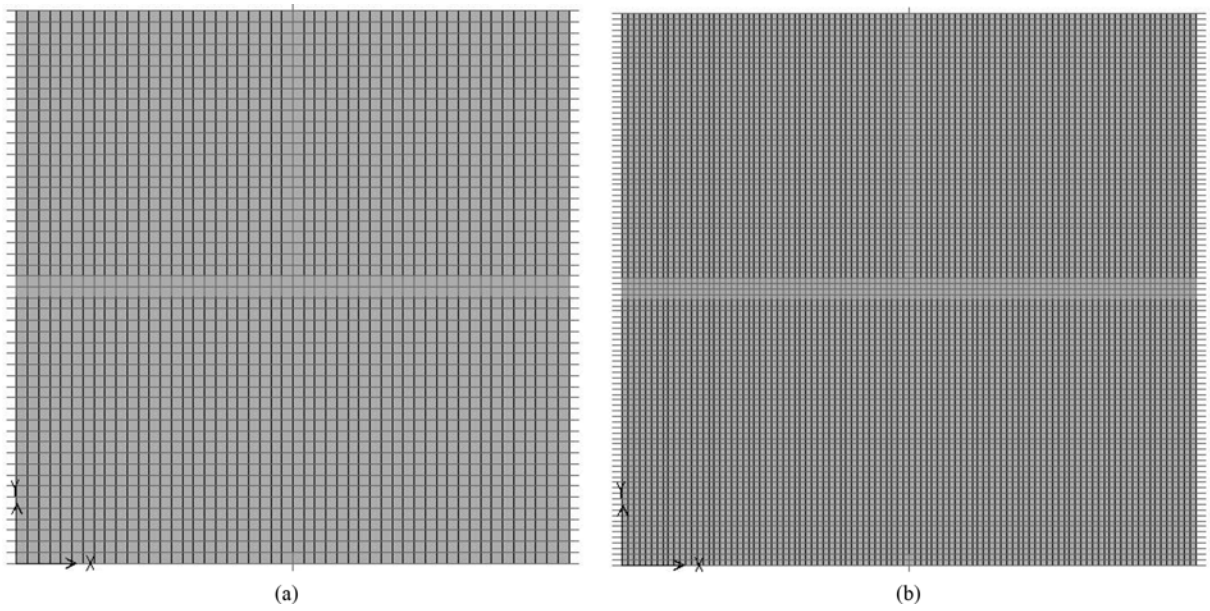

Fig. 3. Plate with Different Mesh Sizes: (a) Model A (50 × 50), (b) Model D (100 × 100)

Table 2. Description of the Basic Random Variables for the Plate on an Elastic Foundation

Variable	Mean	Distribution	COV*
K (kip/ft^3)	800	Normal	0.1 (Timm *et al*., 1998)
P (kips)	50	Normal	0.1 (Besterfield *et al*., 1990)
E (kip/in^2)	29000	Normal	0.076 (Hess *et al*., 2002)

*COV: coefficient of variation

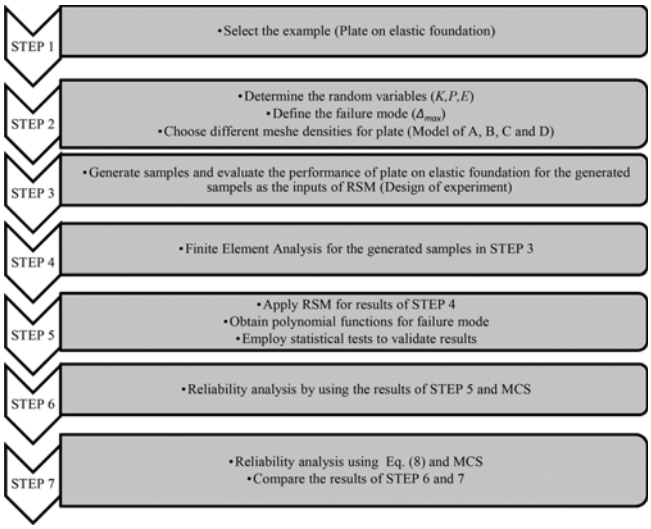

Fig. 4. The Overall View of the Proposed Framework

RSM results were accurate for the reliability evaluation of the plate, the results of the obtained functions were compared with those obtained by the FEM models and validated by the R^2 test. Then, the reliability analyses were done by employing the obtained RSM functions (for each FE mesh density) and MCS.

Comparing the result of the above-mentioned analytical solution with those provided by combining RSM and FEM could be a good framework to examine the effect of mesh density on the reliability assessment of the plate on an elastic foundation. Fig. 4 presents the proposed steps as a flowchart for easier comprehension.

Table 4. The Coefficient of Determination

Model		FEM	Analytical Solution
		R^2	R^2
RSM	A	0.9981	0.9963
	B	0.9950	0.9976
	C	0.9979	0.9993
	D	0.9994	0.9993

3.1.1 The Accuracy of the RSM Results

Table 3 shows the functions governed by RSM for the maximum deflection in different mesh densities. The obtained results were compared with the results of the FEA software and the analytical solution in Eq. (7). For this, the R^2 test was employed. The results have been shown in Table 4. The results of this table were calculated by 100 FEA simulations due to the convergence in their numbers, as shown in Fig. 5. This figure shows that after 70 FEA the trend of convergence is approximately constant and accuracy difference between 90 FEA and 100 FEA is small. As Table 4 shows, the R^2 of the function, obtained from the RSM for model A, are 0.9981 and 0.9963 respectively for FEA and the analytical solution. The R^2 shows a good agreement for the RSM functions between the FEA and the analytical solution. Figs. 6 and 7 show the accuracy of the RSM achieved on model D by the FEA and the analytical solution respectively.

Table 5 presents the maximum deflection in the plate (Δ_{plate}), compared with the analytical solution at the mean point. The results show acceptable responses, as presented by the R^2 test in Table 4. In Table 5, the mean of the abbreviation of RSM-A is the function determined by the response surface methodology for model A. For example, the error percentage for RSM-A is 11.71%. The function results show an acceptable comparison with the analytical results. Increased meshing improves the

Table 3. The Coefficient of the Functions for Maximum Deflection Evaluation

$$\Delta_{plate} = a + \sum_{i=1}^{n} b_i X_i + \sum_{i=1}^{n} c_i X_i^2 + \sum_{i=1}^{n-1} \sum_{j=i+1}^{n} d_{ij} X_i X_j$$

Coefficient	A	B	C	D
a	0.173655010411429	0.183865878823877	0.193320708225335	0.192358540998671
b_1	-0.000229310553236	-0.000238694714471	-0.000236804097006	-0.000251935595379
b_2	0.006334666627792	0.006536655449108	0.007002581739217	0.007326188317855
b_3	-0.000005554631030	-0.000005619877543	-0.000006657043544	-0.000006603425861
c_1	0.000000106897741	0.000000110712893	0.000000108549264	0.000000120457482
c_2	-0.000001512253715	0.000000302802296	-0.000001687106917	-0.000001397628972
c_3	0.000000000069275	0.000000000064504	0.000000000086258	0.000000000084949
d_{12}	-0.000001997051038	-0.000002118551930	-0.000002027598418	-0.000002261957262
d_{13}	0.000000001545942	0.000000001746478	0.000000001631589	0.000000001825651
d_{23}	-0.000000046460024	-0.000000048214441	-0.000000055926936	-0.000000059813297

X_1 : Subgrade modulus (K)
X_2 : Point load (P)
X_3 : Modulus of elasticity (E)

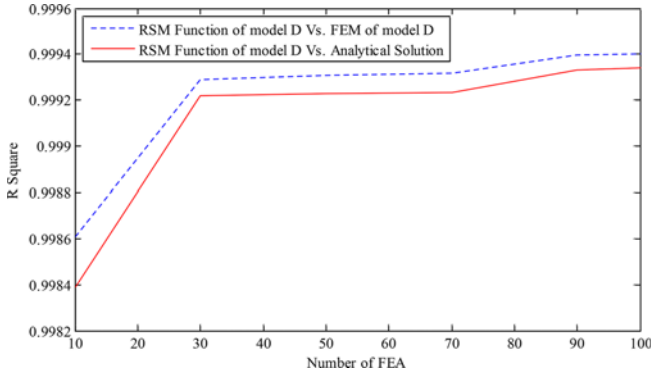

Fig. 5. Accuracy Convergence for the Number of FEAs

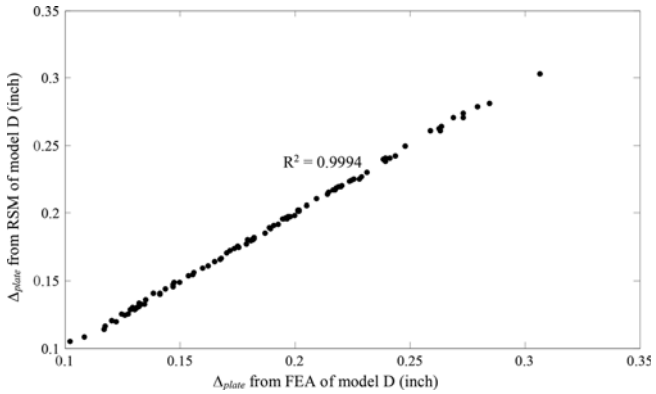

Fig. 6. Comparison of the Results Obtained by RSM and FEM for Model D

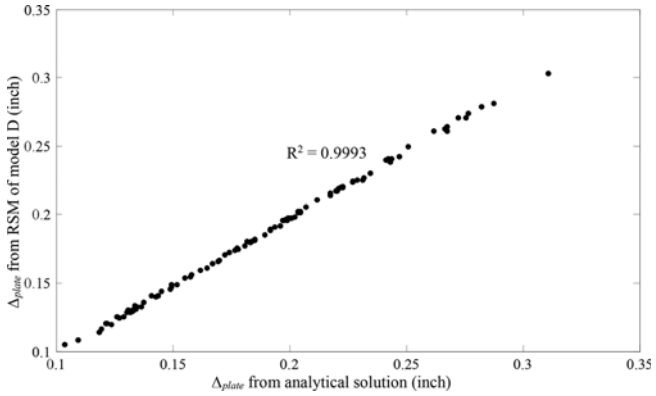

Fig. 7. Comparison of the Results Obtained by RSM and the Analytical Solution for Model D

comparison and the convergence of the models. Fig. 8 shows this too. But, as mentioned in Section 1, engineers and researchers usually accept minor errors due to the optimal CPU time. Table 6 shows the computation time for each FE model, and the percentage difference of time for each model in comparison with the finest mesh (model D). This table shows that the CPU time for model D is fourfold compared with model A. But model A has 75% higher computation time than model D.

3.1.2 Reliability Results

By using RSM, a function was obtained for each model. This function was used in Eq. (8) as the limit-state function to evaluate the reliability of the plate for different mesh densities. Then, the results were compared with the accurate solution provided by the analytical solution determined by Eq. (7).

The reliability index (β) and the PF calculated by MCS, LHS, FORM, and SORM for the plate are shown in Table 7 and Fig. 9. Table 7 shows that the common FORM and SORM present solutions close to the MCS. Hence, they could be used for the reliability analysis of the plate with good accuracy. Moreover, there are fewer samples in LHS compared with the MCS. The mesh density's effects on the reliability evaluation of the problem were unexpected and noticeable. The accurate failure probability, obtained by using MCS and Eq. (7), was 1.42×10^{-3}. However, though it was concluded that all the FEM models (A to D) provided a good approximation of the plate performance, the finest mesh ($100 \times 100 \times 1$) among these models presented the proper reliability index for the plate. As Fig. 9 shows, the error in the failure probability approximation for model A, compared with the analytical function ($PF = 1.42 \times 10^{-3}$), is about 100% (more than that of one unit difference in the reliability index). But, the amount of deflection at the mean point had a roughly acceptable similarity with the accurate solution about 11%. It had a good difference with the previous model ($40 \times 40 \times 1$) and the

Table 5. The Deflection of the Plate at Mean Values (K = 800 kip/ft3, P = 50 kips, E = 29000 kip/in2) for the Different Models

Function	Δ_{plate} (inch)	Percent Error
Analytical Solution	0.178	----------
RSM-A	0.157	11.71%
RSM-B	0.168	5.47%
RSM-C	0.174	2.15%
RSM-D	0.176	1.37%

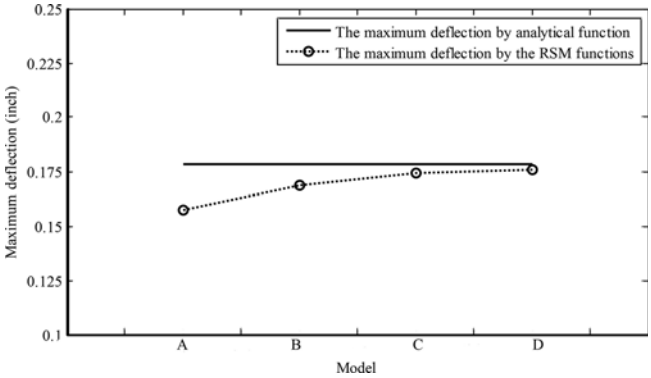

Fig. 8. The Convergence of Δplate at the Mean Point

Table 6. Analysis of the CPU time for FE Models

FE Model	CPU time (second)	Difference
A	7	75%
B	14	50%
C	23	17.86%
D	28	----------

Table 7. Reliability Results for the Plate on an Elastic Foundation

Failure limit ($\Delta_{allowable}$)	Function		β (MCS) NoS = 10000000	PF (MCS) NoS = 10000000	β (LHS) NoS = 6500000	PF (LHS) NoS = 6500000	β (SORM)	PF (SORM)	β (FORM)	PF (FORM)
0.25 (inch)	Δ_{plate}	RSM-A	4.12	1.87×10^{-5}	4.13	1.80×10^{-5}	4.12	1.87×10^{-5}	4.13	1.79×10^{-5}
		RSM-B	3.48	2.49×10^{-4}	3.48	2.46×10^{-4}	3.48	2.49×10^{-4}	3.49	2.44×10^{-4}
		RSM-C	3.17	7.56×10^{-4}	3.17	7.50×10^{-4}	3.17	7.56×10^{-4}	3.18	7.24×10^{-4}
		RSM-D	3.05	1.15×10^{-3}	3.06	1.10×10^{-3}	3.05	1.15×10^{-3}	3.06	1.11×10^{-3}
		Analytical Function	2.98	1.42×10^{-3}	2.99	1.40×10^{-3}	2.99	1.40×10^{-3}	3.01	1.30×10^{-3}

*NoS: Number of Samples

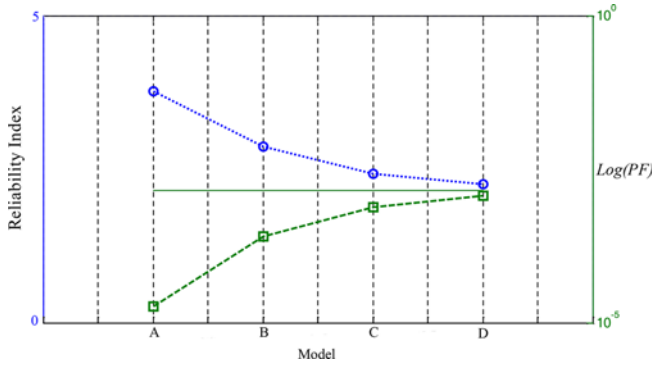

Fig. 9. The Convergence of the Reliability Index of the Plate on the Elastic Foundation

Table 8. The Effect of Mesh Density on the Reliability Evaluation of the Plate

Function	The percent error of deflection value at the mean point	The error in the probability of failure approximation	The differences of reliability index with the correct value
RSM-A	11.71%	98.68%	1.14
RSM-B	5.47%	82.46%	0.50
RSM-C	2.15%	46.69%	0.19
RSM-D	1.37%	18.69%	0.06

next model (60 × 60 × 1). It also had an acceptable difference with the analytical results. Table 8 gives a more comprehensive comparison of the effects of mesh density. It shows that compared with the theoretical solution, the determined error in the maximum deflection evaluation for every model is minor. For instance, RSM-B has about 5% error at the mean point for the calculation of the Δ_{plate}. But the difference in the evaluated failure probability is about 82%. Hence, if the maximum difference in the reliability index approximation of the problem is less than 20%, only models C and D satisfy the criteria. Hence, it was found that the acceptance range in the convergence step to choose a proper mesh density should be reduced to 2% to determine the reliability index for the problem with an acceptable accuracy.

3.1.3 Reliability-based Sensitivity Results

Table 9 gives the results of the sensitivity analysis. The results were calculated by the failure limit given in Table 7. Table 9 shows the sensitivity measures in terms of the partial derivation of the failure probability with respect to the mean value, standard deviation, and the multiplied standard deviation of the parameters. The negative values can be explained by the fact that an increase in the related parameter decreases the probability of failure. Table 9 shows that the second parameter (central load) is the more important variable in the variation of the mean and the standard deviation. This conclusion was proved in all the five functions. Also, this table shows that the mesh density does not have a noticeable effect on the sensitivity results for the ranking of parameters (bold cells are the most important parameters). The accuracy of the sensitivity results provided by FEA are not greatly different from the theoretical results provided by Eq. (7). Hence, the accuracy of the obtained sensitivity results provided by employing FEM is guaranteed.

3.1.4 Change of the Allowable Deflection Value (failure limit)

In this section, the PF is calculated by the MCS for the analytical and the RSM functions by changing the allowable deflection value (failure limit). The results show that by changing the failure

Table 9. MCS Sensitivity Results for the Plate Models with Different Mesh Densities

Sensitivity type	MCS reliability-based sensitivity results				
	Analytical function	RSM-A	RSM-B	RSM-C	RSM-D
$(\partial PF / \partial \mu_{X1})\times \sigma_{X1}$	-26.00×10^{-4}	-0.5512×10^{-4}	-5.236×10^{-4}	-14.00×10^{-4}	-20.00×10^{-4}
$(\partial PF / \partial \mu_{X2})\times \sigma_{X2}$	35.00×10^{-4}	0.6637×10^{-4}	7.023×10^{-4}	20.00×10^{-4}	28.00×10^{-4}
$(\partial PF / \partial \mu_{X3})\times \sigma_{X3}$	-18.00×10^{-4}	-0.3025×10^{-4}	-3.287×10^{-4}	-10.00×10^{-4}	-14.00×10^{-4}
$(\partial PF / \partial \sigma_{X1})\times \sigma_{X1}$	12.02×10^{-2}	0.38×10^{-2}	2.79×10^{-2}	6.31×10^{-2}	9.42×10^{-2}
$(\partial PF / \partial \sigma_{X2})\times \sigma_{X2}$	345.97×10^{-2}	8.70×10^{-2}	80.00×10^{-2}	208.08×10^{-2}	287.87×10^{-2}
$(\partial PF / \partial \sigma_{X3})\times \sigma_{X3}$	0.21×10^{-2}	00.00×10^{-2}	0.04×10^{-2}	0.12×10^{-2}	0.17×10^{-2}

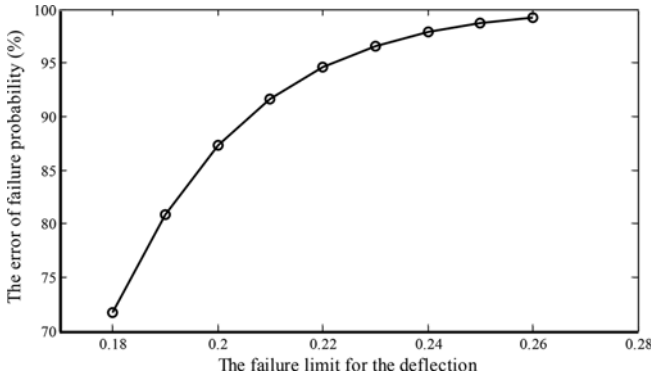

Fig. 10. Error Percentage of Failure Probability in Different Failure Limits between the Analytical Function and RSM-A

limit in Eq. (8), the error percentage between the analytical function and the RSM-A is intensely raised. Fig. 10 shows that by increasing the failure limit, the error percentage between RSM-A and the analytical function rises too. It shows that if the choice of a failure limit is closer to the safe region, the results obtained from a model with fewer meshes will be more unreliable. Besides, this figure also presents the estimated functions obtained by RSM to acquire the real failure probability. Three types of functions—first, second, and third order—are employed in Fig. 10. It shows that the third order by $R^2 = 0.999$, which is calculated by the analytical function and RSM-A, is placed on the error values. Table 10 shows the required coefficients of the function of Eq. (10). In consequence, an equation is presented for calculating the correct probability of failure for this specific mesh density (50 × 50 × 1) in Eq. (11). This equation can provide the correct *PF* for model A at different failure limits. This means that if model A, with a specific failure limit, is analyzed to get the *PF* (PF_{model}), Eq. (11) can estimate the correct *PF* (PF_{real}) close to that of the analytical function.

Table 10. The Coefficient of the Function for Correcting The *PF* Model

Coefficient	
a	$-0.094535960417770\times10^4$
b	$1.244420648023752\times10^4$
c	$-4.974120216162062\times10^4$
d	$6.666638137206058\times10^4$

Table 11. R^2 test in Different Orders of Estimating the Correct PF

Order of estimated function for correct *PF*	R^2
1	0.8478357
2	0.9908708
3	0.9997970
4	0.9999957
5	0.9999958
6	0.9999992
7	0.9999999
8	1

$$\%Error = a + b\times\Delta_{\text{allowable}} + c\times\Delta^2{}_{\text{allowable}} + d\times\Delta^3{}_{\text{allowable}} \quad (10)$$

$$PF_{real} = \left(1+\frac{\%Error}{100}\right)\times PF_{model} \quad (11)$$

To estimate the correct failure probability, the accuracy of the different orders was compared by employing the R^2 test. Table 11 shows the results. According to this table, the accuracy of the second order is acceptable enough, and for the eighth order, R^2 is 1.

3.2 Cylindrical Storage Tank

In this section, a cylinder is analyzed for its internal pressure load. For this structure, three main failure modes were taken into account for reliability evaluation. These were "exceeding the radial outward displacement" ($u1$), "vertical displacement at the top of the cylinder" ($u3$), and "stress" (S_{11}). These were considered as the limit-state functions of the problem. The analytical solutions to determine S_{11}, $u1$, and $u3$ can be presented as (Young and Budynas, 2001):

$$S_{11} = \frac{P\times r}{t} \quad (12)$$

$$u3 = \frac{P\times r\times\upsilon\times h}{E\times t} \quad (13)$$

$$u1 = \frac{P\times r^2}{E\times t} \quad (14)$$

To provide the FEM-based performance of the structure, it was modeled as a cylinder with a height (h) of 200 inches and a radius (r) of 60 inches. Internal pressure (P), the modulus of elasticity (E), and thickness (t) were considered to be the random variables of the problem. These are shown in Table 12. The material used in this study was steel with a modulus of elasticity $E = 29{,}000$ kip/in^2 and Poisson's ratio, $\upsilon = 0.3$.

To analyze the effect of the mesh density on the reliability analysis, the cylinder was modeled in four different mesh sizes, namely E, F, G, and H, with 4 × 8, 8 × 16, 12 × 24, and 24 × 48 meshes (height × circumference) respectively. Two models are presented in Fig. 11.

The RSM results' validation and the reliability evaluation for the cylindrical storage tank were performed following the framework of the previous problem. Tables 13 to 17 and Fig. 12 present the results. Since the performed steps have been presented in detail in the previous example, the results are only being summarized for this problem.

Appendix A shows the functions obtained by RSM for the cylinder failure modes. Similar to the previous example, Table

Table 12. Description of the Basic Random Variables for the Cylindrical Storage Tank

Variable	Mean	Distribution	COV
P (kip/in^2)	1	Normal	0.1 (Amirat *et al*., 2006)
E (kip/in^2)	29000	Normal	0.076 (Hess *et al*., 2002)
t (inch)	1	Lognormal	0.0417 (Hess *et al*., 2002)

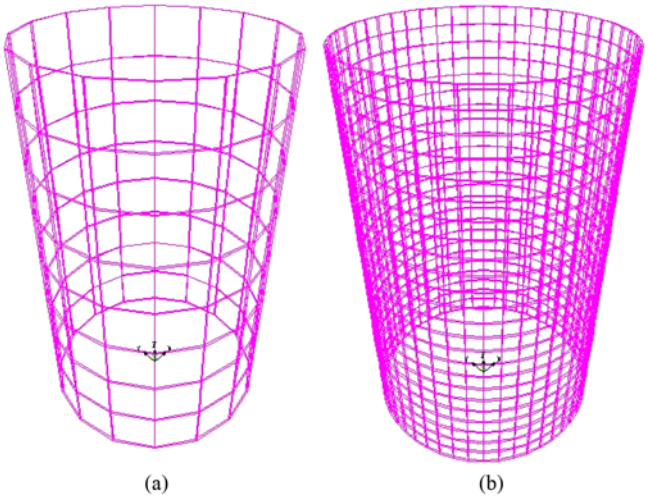

Fig. 11. Cylindrical Storage Tank with Different Mesh Sizes: (a) Model F (8 × 16), (b) Model H (24 × 48)

Table 13. The Coefficient of Determination for the Cylinder

Model		FEM			Analytical Solution		
		R^2			R^2		
		S_{11}	$u1$	$u3$	S_{11}	$u1$	$u3$
RSM	E	1	0.9993	0.9993	1	0.9993	0.9993
	F	0.9999	0.9950	0.9950	1	0.9989	0.9990
	G	1	0.9993	0.9993	1	0.9993	0.9993
	H	1	0.9993	0.9993	1	0.9993	0.9993

Table 14. Results at Mean Values for the Cylinder (P = 1 kip/in2, E = 29000 kip/in2, t = 1 in)

Function	S_{11}		$u1$		$u3$	
	Value (kip/in^2)	Error (%)	Value (inch)	Error (%)	Value (inch)	Error (%)
Analytical Solution	60	---------	0.124	---------	0.124	---------
RSM-E	55.415	7.64%	0.115	7.08%	0.115	7.08%
RSM-F	58.786	2.02%	0.122	1.86%	0.122	1.86%
RSM-G	59.468	0.89%	0.124	0.29%	0.124	0.29%
RSM-H	59.853	0.24%	0.125	-0.35%	0.125	-0.35%

13 shows the RSM, with R^2 equal to 0.999 for each model of failure mode, which provides the accurate performance functions to predict the performance of the tank to evaluate the reliability. Table 14 indicates that the error at the mean point for each RSM function satisfies commonly acceptable ranges of errors compared with the theoretical values.

Table 16. The Effect of Mesh Density on the Reliability Analysis of the Cylinder

Failure mode	Function	The percent error of failure mode value at the mean point	The error in the probability of failure approximation	The differences of reliability index with the correct value
S_{11}	RSM-E	7.64%	97.90%	0.98
	RSM-F	2.02%	63.83%	0.28
	RSM-G	0.89%	36.66%	0.13
	RSM-H	0.24%	17.69%	0.06
$u1$	RSM-E	7.08%	93.45%	0.65
	RSM-F	1.86%	42.70%	0.14
	RSM-G	0.29%	16.37%	0.046
	RSM-H	-0.35%	-3.98%	0.01
$u3$	RSM-E	7.08%	94.54%	0.69
	RSM-F	1.86%	40.88%	0.13
	RSM-G	0.29%	17.85%	0.05
	RSM-H	-0.35%	-2.80%	0.01

Table 15 proves the sensitivity of the mesh density on the reliability evaluation. Table 16 shows the amounts of difference among the models with an analytical solution. For instance, in the stress mode (S_{11}), the error in the failure probability estimation for model E, compared with the analytical function, is about 100% (close to one unit difference in the reliability index). But, the amount of stress at the mean point had a roughly acceptable similarity with the accurate solution—about 7.6%. Furthermore, the 2% error, known as the "tinge of error" from a deterministic viewpoint, had about 64% error in the approximation of the *PF* for the stress function, and 43% for the displacement function. Fig. 12 also shows the trend of convergence of the reliability index to the exact value in the three failure modes.

The MCS sensitivity resulting from the cylinder failure modes also proves the conclusion of the previous problem. Fig. 13 shows that by changing the failure limit in the performance function of the three failure modes, the error percentage between the analytical functions and the RSM-E is intensely raised.

4. Conclusions

The selection of a suitable mesh density for the reliability analysis of systems whose performance evaluation requires FEA is a challenge that is yet to be covered. This paper evaluated the reliability of two common engineering problems by using four

Table 15. The Reliability Results for the Cylinder by MCS (NoS = 15000000)

Function			Analytical Function	RSM-E	RSM-F	RSM-G	RSM-H
Failure mode	Allowable value	Reliability result					
S_{11}	82 (kip/in^2)	*PF*	67.75×10^{-5}	14.20×10^{-6}	24.51×10^{-5}	42.91×10^{-5}	55.76×10^{-5}
$u1$	0.20 (inch)	*PF*	12.56×10^{-5}	8.00×10^{-6}	71.90×10^{-6}	10.50×10^{-5}	13.06×10^{-5}
$u3$	0.20 (inch)	*PF*	12.62×10^{-5}	6.90×10^{-6}	74.60×10^{-6}	10.36×10^{-5}	12.97×10^{-5}

*NoS: Number of Samples

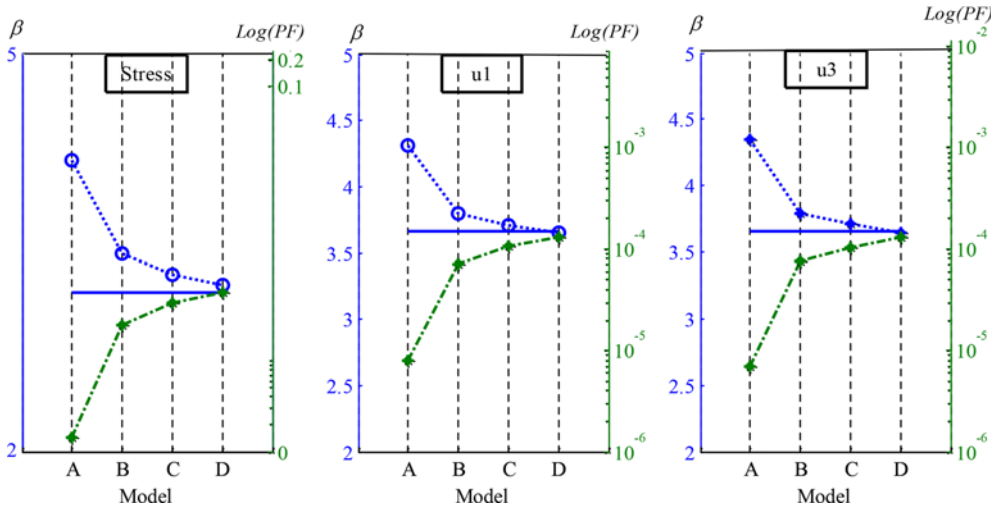

Fig. 12. The Convergence of the Reliability Index for the Cylinder Failure Modes

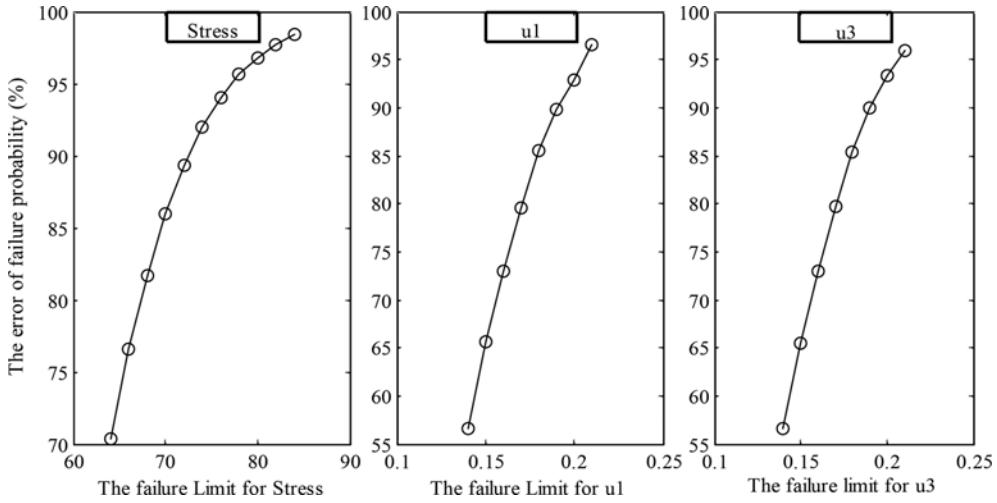

Fig. 13. The Error Percentage of the Failure Probability at Different Failure Limits between the Analytical Function and RSM-E for the Three Failure Modes of the Cylinder

FEM-based models. The difference between the proposed models for each problem was just in their mesh densities. The selected models presented an acceptable performance evaluation from the viewpoint of a deterministic performance evaluation. To use MCS for reliability analysis and to reduce the computation cost of simulations, the polynomial RSM was used for each model to provide an explicit performance function (instead of an implicit one that required FEA). The performed R^2 test showed that RSM is a good choice for this purpose. However, a comparison of the reliability evaluation results with the theoretical solution (determined by the analytical solution) showed that though the accuracy of all the models were acceptable from a deterministic viewpoint, mesh density highly affected the reliability results. Only one among the four proposed models could estimate the probability of failure with an acceptable accuracy. Hence, the validation of the FE results should be reduced from 15% to less than 2% to provide proper reliability results. This could be vital, especially for reliability-based design optimization of structures in which mesh density highly affects the safety of the determined optimum solution.

By analyzing the errors produced from the different values of the failure limit, this study also proposes a simple formulation to estimate the errors in the reliability evaluation. It was performed for a model with coarse mesh density (model A), but could be performed for the other inaccurate models. Furthermore, the comparison of the reliability-based sensitivity results in the accurate solution indicates that the mesh density of the models does not highly affect the sensitivity results provided by FEA.

References

Amirat, A., Mohaned-Chateauneuf, A., and Chaoui, K. (2006). "Reliability assessment of underground pipelines under the combined effect of active corrosion and residual stress." *International Journal of Pressure Vessels and Piping,* Vol. 83, No. 2, pp. 107-117, DOI: 10.1016/j.ijpvp.

Ashford, S. A. and Sitar, N. (2001). "Effect of element size on the static finite element analysis of steep slopes." *Int. J. Numer. Anal. Meth. Geomech*., Vol. 25, No. 14, pp. 1361-1376, DOI: 10.1002/nag.184.

Besterfield, G. H., Liu, W. K., Lawrence, M., and Belyschko, T. (1990). "Brittle fracture reliability by probabilistic finite elements." *J. Eng. Mech. ASCE,* Vol. 116, No. 3, pp. 642-659, DOI: 10.1061/(ASCE) 0733-9399(1990)116:3(642).

Box, G. E. P. (1954). "The exploration and exploitation of response surfaces: Some general considerations and examples." *Biometrics,* Vol. 10, No. 1, pp. 16-60, DOI: 10.2307/3001663.

Brown, P. R. (1981). "A non-interactive method for the automatic generation of finite element meshes using the Schwarz-Christoffel transformation." *Comput. Methods Appl. Mech. Engrg.,* Vol. 25, No. 1, pp. 101-126, DOI: 10.1016/0045-7825(81)90071-2.

Bucher, C. G. and Bourgund, U. (1990). "A fast and efficient response surface approach for structural reliability problems." *Structural Safety*, Vol. 7, No. 1, pp. 57-66, DOI: 10.1016/0167-4730(90)90012-E.

Der kiureghian, A. and Ke, J. B. (1998). "The stochastic finite element method in structural reliability." *Probabilistic Engineering Mechanics,* Vol. 3, No. 2, DOI: 10.1016/0266-8920(88)90019-7.

Di Sciuva, M. and Lomario, D. (2003). "A comparison between Monte Carlo and FORMs in calculating the reliability of a composite structure." *Composite Structures,* Vol. 59, No. 1, pp. 155-162, DOI: 10.1016/ S0263-8223(02)00170-8.

Dyck, D. N., Lowther, D. A., and McFee, S. (1992). "Determining an approximate finite element mesh density using neural network techniques." *IEEE Transactions on Magnetics,* Vol. 28, No. 2, pp. 1767-1770, DOI: 10.1109/20.124047.

Faravelli, L. (1989). "Response surface approach for reliability analyses." *J. Eng. Mech. ASCE*, Vol. 115, No. 2, pp. 2763-2781, DOI: 10.1061/ (ASCE)0733-9399(1989)115:12(2763).

Ghohani-Arab, H. and Ghasemi, M. R. (2015). "A fast and robust method for estimating the failure probability of structures." *P. I. Civil. Eng. Str B,* Vol. 168, No. 4, pp. 298-309, DOI: 10.1680/stbu. 13.00091.

Gray, H. A., Taddei, F., Zavatsky, A. B., Cristofolini, L., and Gill, H. S. (2008). "Experimental validation of a finite element model of a human cadaveric tibia." *Journal of Biomechanical Engineering,* Vol. 130, No. 3, DOI: 10.1115/1.2913335.

Hamdia, K. M., Msekh, M. A., Silani, M., Vu-Bac, N., Zhuang, X., Nguyen-Thoi, T., and Rabczuk, T. (2015). "Uncertainty quantification of the fracture properties of polymeric nanocomposites based on phase field modeling." *Composite Structures*, Vol. 133, pp. 1177-1190, DOI: 10.1016/j.compstruct.2015.08.051.

Helton, J. C. and Davis, F. J. (2003). " Latin hypercube sampling and propagation of uncertainty in analysis of complex system." *Reliability Engineering and Safety*, Vol. 81, No. 1, pp. 23-69, DOI: 10.1016/ S0951 8320(03)00058-9.

Hess, P., Bruchman, D., Assakkaf, I., and Ayyub, B. (2002). "Uncertainties in material strength, geometric and load variables." *Naval Engineering Journal*, Vol. 114, No. 2, pp. 139-166, DOI: 10.1111/j.1559-3584. 2002.tb00128.x.

Hu, K. and Zhang, Y. J. (2016). "Centroidal Voronoi tessellation based polycube construction for adaptive all-hexahedral mesh generation." *Comput. Methods Appl. Mech. Engrg.,* Vol. 305, pp. 405-421, DOI: 10.1016/j.cma.2016.03.021.

Hurtado, J. E. and Barbat, A. H. (1998). "Monte Carlo techniques in computational stochastic mechanics." *Archives of Computational in Engineering,* Vol. 5, No. 1, pp. 3-30, DOI: 10.1007/BF02736747.

Idelsohn, S.R., Onate, E. (2006). "To mesh or not to mesh. That is the question…." *Comput. Methods Appl. Mech. Engrg.,* Vol. 195, Nos. 37-40, pp. 4681-4696, DOI: 10.1016/j.cma.2005.11.006.

Jensen, H. A., Mayorga, F., and Papadimitriou, C. (2015). "Reliability sensitivity analysis of stochastic finite element models." *Comput. Methods Appl. Mech. Engrg.,* Vol. 296, pp. 327-351, DOI: 10.1016/ j.cma.2015.08.007.

Jones, A. C. and Wilcox, R. K. (2008). "Finite element analysis of the spine: Towards a framework of verification, validation and sensitivity analysis." *Medical Engineering & Physics*, Vol. 30, No. 10, pp. 1287-1304, DOI: 10.1016/j.medengphy.2008.09.006.

Li, L. and Sun, L. (2016). "Experimental and numerical of crack behavior and life prediction of 18Cr2Ni4WA steel subjected to repeated impact loading." *Engineering Failure Analysis,* Vol. 65, pp. 11-25. DOI: 10.1016/j.engfailanal.2016.03.018.

Li, Z., Kindig, M. W., Subit, D., and Kent, R. W. (2010). "Influence of mesh density, cortical thickness and material properties on human rib fracture prediction." *Medical Engineering & Physics*, Vol. 32, No. 9, pp. 998-1008, DOI: 10.1016/j.medengphy.2010.06.015.

Lopez, R. H., Miguel, L. F. F., Belo, I. M., and Souza Cursi, J. E. (2014). "Advantages of employing a full characterization method over FORM in the reliability analysis of laminated composite plates." *Composite Structures,* Vol. 107, pp. 635-642, DOI: 10.1016/j.compstruct. 2013.08.024.

Melchers, R. E. (1999). *Structural reliability analysis and prediction*, Chichester: John Wiley & Sons.

Moxey, D., Green, M. D., Sherwin, S. J., and Peiro, J. (2015). "An isoparametric approach to high-order curvilinear boundary-layer meshing." *Comput. Methods Appl. Mech. Engrg*., Vol. 283, pp. 636-650, DOI: 10.1016/j.cma.2014.09.019.

Myers, R., Montgomery, D., and Anderson-cook, C. (2009). *Response surface methodology*, John Wiley & Sons.

Nowak, A. S. and Collins, K. R. (2000). *Reliability of structures*, McGraw-Hill, New York.

Pasbani Khiavi, M. (2016). "Investigation of the effect of reservoir bottom absorption on seismic performance of concrete gravity dams using sensitivity analysis." *KSCE Journal of Civil Engineering*, Vol. 20, No. 5, pp. 1977-1986, DOI: 10.1007/s12205-015-1159-5.

Perillo-Marcone, A., Alonso-Vazquez, A., and Taylor, M. (2003). "Assessment of the effect of mesh density on the material property discretisation within QCT based FE models: A practical example using the implanted proximal tibia." *Computer Methods in Biomechanics and Biomedical Engineering,* Vol. 6, No. 1, pp. 17-26, DOI: 10.1080/ 1025584031000064470.

Rashki, M., Miri, M., and Azhdary-Moghadam, M. (2012). "A new efficient simulation method to approximate the probability of failure and most probable point." *Structural Safety*, Vol. 39, pp. 22-29, DOI: 10.1016/j.strusafe.2012.06.003.

Roth, S. and Oudry, J. (2009). "Influence of mesh density on a finite element model under dynamic loading." *Proceedings of 3rd European Hyperworks Technology Conference,* November 2nd-4th, Ludwigsburg, Germany.

Timm, D., Birgisson, B., and Newcomb, D. (1998). "Variability of mechanistic-empirical flexible pavement design parameters." *Proceedings of the Fifth International Conference on the Bearing Capacity of Roads and Airfields,* Vol. 1, Norway, pp. 629-638.

Timoshenko, S. and Woinowsky-Krieger, S. (1959). *Theory of plates and shells*, McGraw-Hill.

Waide, V., Cristofolini, L., Stolk, J., Verdonschot, N., Boogaard, G. J., and Toni, A. (2004). "Modeling the fibrous tissue layer in cemented hip replacement: finite element methods." *J. Biomech,* Vol. 37, No. 1,

pp. 13-26, DOI: 10.1016/S0021-9290(03)00258-6.
Xu, T., Xiang, T., Zhao, R., Yang, G., and Yang, Ch. (2016). "Stochastic analysis on flexural behavior of reinforced concrete beams based on piecewise response surface scheme." *Engineering Failure Analysis,* Vol. 59, pp. 211-222, DOI: 10.1016/j.engfailanal.2015.10.004.
Yao, Sh., Zhang, D., Chen, X., Lu, F., and Wang, W. (2016). "Experimental and numerical study on the dynamic response of RC slabs under blast loading." *Engineering Failure Analysis*, Vol. 66, pp. 120-129, DOI: 10.1016/j.engfailanal.2016.04.027.
Young, W. C. and Budynas, R. G. (2001). *Roark's formulas for stress and strain,* McGraw-Hill.
Zhao, Y. G. and Ono, T. (2001). "Moment methods for structural reliability." *Structural Safety,* Vol. 23, No. 1, pp. 47-75, DOI: 10.1016/S0167-4730(00) 00027-8.
Zmudzki, J., Walke, W., and Chladek, W. (2008). "Influence of model discretization density in FEM numerical analysis on the determined stress level in bone surrounding dental implants." *Information Tech. in Biomedicine*, ASC, Vol. 47, pp. 559-567, DOI: 10.1007/978-3-540-68168-7_64.

Appendix. Functions Governed by RSM for the Three Failure Modes of the Cylinder

This appendix presents the coefficient of the functions obtained by RSM for the three failure modes of the cylindrical storage tank.

Table 17. The Coefficient of the Functions for Stress in the Cylinder

RSM Function	$s_{11} = a + \sum_{i=1}^{n} b_i X_i + \sum_{i=1}^{n} c_i X_i^2 + \sum_{i=1}^{n-1} \sum_{j=i+1}^{n} d_{ij} X_i X_j$			
Coefficient	E	F	G	H
a	57.2631052530254	58.6919828204379	61.4529866748651	61.8502443536071
b_1	106.3340297687385	112.3180626419321	114.1107159019907	114.8491053984774
b_2	-0.0000659307002	-0.0001373825516	-0.0000707553652	-0.0000711968863
b_3	-108.1276058858434	-108.8712383353530	-116.0393398091599	-116.7901226902796
c_1	0.0502649327228	0.2671059157366	0.0539285673594	0.0542568701910
c_2	0.0000000002870	-0.0000000022250	0.0000000003080	0.0000000003098
c_3	51.2043405348121	48.6760943126588	54.9510768446436	0.0000507910232
d_{12}	-0.0000021566812	-0.0000139383145	-0.0000023120312	-0.0000023292548
d_{13}	-50.9392938389311	-53.6338501687740	-54.6648782677529	-55.0185933976282
d_{23}	0.0000470281075	0.0002619931306	0.0000504683124	55.3067450915660

X_1 : Uniform internal pressure (P)
X_2 : Modulus of elasticity (E)
X_3 : Thickness (t)

Table 18. The Coefficient of the Functions for $u1$ in the Cylinder

RSM Function	$u1 = a + \sum_{i=1}^{n} b_i X_i + \sum_{i=1}^{n} c_i X_i^2 + \sum_{i=1}^{n-1} \sum_{j=i+1}^{n} d_{ij} X_i X_j$			
Coefficient	E	F	G	H
a	0.535660913119938	0.602503561476942	0.574877769566934	0.578577926574307
b_1	0.347338036171397	0.386023255556990	0.372733137619838	0.375147982435001
b_2	-0.000010785243491	-0.000010643345591	-0.000011573927243	-0.000011648854397
b_3	-0.737585847720284	-0.890606780833325	-0.791602347758417	-0.796690086677867
c_1	-0.001830633848054	-0.003210586199781	-0.001964313551837	-0.001977118386553
c_2	0.000000000125207	0.000000000169850	0.000000000134365	0.000000000135233
c_3	0.314538998467693	0.433769752800496	0.337575695231366	0.339744606245281
d_{12}	-0.000003712247571	-0.000003810995186	-0.000003983734688	-0.000004009477877
d_{13}	-0.116929651596474	-0.141242902269712	-0.125475095267010	-0.126290702720349
d_{23}	0.000003078591261	0.000000376625711	0.000003303609233	0.000003325070665

X_1 : Uniform internal pressure (P)
X_2 : Modulus of elasticity (E)
X_3 : Thickness (t)

Table 19. The Coefficient of the Functions for *u*3 in the Cylinder

RSM Function	$u3 = a + \sum_{i=1}^{n} b_i X_i + \sum_{i=1}^{n} c_i X_i^2 + \sum_{i=1}^{n-1} \sum_{j=i+1}^{n} d_{ij} X_i X_j$			
Coefficient	E	F	G	H
a	0.535660913119938	0.602503561476942	0.574877769566934	0.578577926574307
b_1	0.347338036171397	0.386023255556990	0.372733137619838	0.375147982435001
b_2	-0.000010785243491	-0.000010643345591	-0.000011573927243	-0.000011648854397
b_3	-0.737585847720284	-0.890606780833325	-0.791602347758417	-0.796690086677867
c_1	-0.001830633848054	-0.003210586199781	-0.001964313551837	-0.001977118386553
c_2	0.000000000125207	0.000000000169850	0.000000000134365	0.000000000135233
c_3	0.314538998467693	0.433769752800496	0.337575695231366	0.339744606245281
d_{12}	-0.000003712247571	-0.000003810995186	-0.000003983734688	-0.000004009477877
d_{13}	-0.116929651596474	-0.141242902269712	-0.125475095267010	-0.126290702720349
d_{23}	0.000003078591261	0.000000376625711	0.000003303609233	0.000003325070665

X_1 : Uniform internal pressure (P)
X_2 : Modulus of elasticity (E)
X_3 : Thickness (t)